Environmental and Economic Characteristics of Electrofuel Production Pathways

by

Stewart Anthony Isaacs

B.S., Stanford University (2017)

Submitted to the Department of Aeronautics and Astronautics
in partial fulfillment of the requirements for the degree of

Master of Science in Aeronautics and Astronautics

at the

MASSACHUSETTS INSTITUTE OF TECHNOLOGY

June 2019

Signature redacted

Author .....
Department of Aeronautics and Astronautics
May 23, 2019

Signature redacted

Certified by .....
Steven R.H. Barrett
Associate Professor of Aeronautics and Astronautics
Thesis Supervisor

Signature redacted

Accepted by .....
Sertac Karaman
Associate Professor of Aeronautics and Astronautics
Chair, Graduate Program Committees

Environmental and Economic Characteristics of Electrofuel Production Pathways

by

Stewart Anthony Isaacs

Submitted to the Department of Aeronautics and Astronautics
on May 23, 2019, in partial fulfillment of the
requirements for the degree of
Master of Science in Aeronautics and Astronautics

Abstract

Electrofuels are liquid fuels derived from CO_2 and electricity, which have the potential to store intermittent renewable power and reduce transportation's climate impact. In this work, I assess the economic and environmental characteristics of four technology pathways for electrofuel production, using the methods of life cycle analysis and techno- economic assessment. In addition, the analysis includes a number of scenarios in which the technologies are powered directly from dedicated renewable electricity generation. The results indicate that the hybrid power- and biomass-to-liquids (PBtL) pathway may represent a promising option for electrofuel production in terms of lifecycle emissions reductions and minimum selling price. I further characterize the PBtL pathway by combining spatially-resolved data on biomass cultivation, electricity generation, and cost-optimized solar-hydrogen production in the United States (US). I find that the resulting fuel would have a minimum selling price between \$2.10 and \$3.81 per liter and lifecycle emissions of 15-27 gCO_2e/MJ depending on the production location.

Thesis Supervisor: Steven R.H. Barrett
Title: Associate Professor of Aeronautics and Astronautics

Acknowledgments

I would first like to thank Professor Steven Barrett for advising my thesis and offering academic guidance and mentorship. I'd also like to thank Dr. Mark Staples for his consistent and detailed support for this research project. I've grown tremendously from our time working together. Additionally, I would like to thank the MIT Energy Initiative and the ENI energy company for supporting this work financially.

My time in LAE has been made much more enjoyable by sharing space with incredible colleagues. Thank you to Prashanth Prakash, Ines Sanz Morere, Thibaud Fritz, Arthur Brown and Yash Dixit for contributing to a welcoming work environment. Special thank you to Juju Wang and Liam Comidy for going through challenging milestones such Quals and thesis research together - both as fuels team members and classmates.

I cannot imagine MIT without the communities I've become deeply invested in including my AeroAfro family, and the BGSA. Thank you for providing me with the fulfillment and moments of joy I needed to make it through rough periods. Finally, I'd like to thank my mentors: Professor Harris, for your sage like wisdom and encouragement to satisfy my soul. And Professor Danielle Wood for inspiring me to see how my skills and research can create a more just world.

Contents

List of Figures

List of Tables

Chapter 1

Introduction and Motivation

Major changes to the way that society produces and uses energy are required to reduce greenhouse gas (GHG) emissions, and mitigate the worst impacts of climate change [1]. Although vehicle electrification is one strategy to reduce emissions, some sectors, such as aviation, trucking and shipping, will be challenging to electrify due to the limitations of battery technologies [2] [3] [4].

Another mitigation strategy is to use low life cycle CO_2 emissions fuels, such as some biofuels, that are compatible with existing combustion-powered vehicles. The aviation industry, for example, has made efforts to enable the use of biofuels to reduce the industry's climate impacts [5]. However, biofuels are not without their own challenges. For example, there are environmental impacts associated with biomass feedstock cultivation, including water consumption and GHG emissions from land use change (LUC) [6] [7]. Biomass-derived liquid fuels are limited in their potential to mitigate emissions due to constraints such as land availability, life cycle emissions including LUC, and competition with food, feed, heat and power production [8].

In contrast, electrofuels offer an alternative method to decarbonize transportation, while making use of excess intermittent electricity from renewable sources. Electrofuels constitute a class of technologies that use power as a primary input to convert carbon from concentrated CO_2 emissions, atmospheric CO_2, or biomass, to liquid hydrocarbon fuels [9]. A number of peer-reviewed studies have proposed various electrofuel production pathways, and have assessed their economic viability or environmental

impacts relative to petroleum- and biomass-derived fuels [10] [2] [11]. In particular, previous analyses suggest that electrofuels technology paired with biomass gasification may have greater land-use and carbon efficiency than conventional biomass-to-liquids fuels [12]. This suggests that electrofuels technologies may hold promise to leverage a limited biomass supply to sustainably meet the energy demands of transportation. Indeed, Blaco et al. (2018) suggest electrofuels (also known as power-to-liquid or power-to-fuels) may play an important role in national decarbonized energy systems [13].

In this analysis I compare several technology pathways for electrofuel production, and quantify how electricity generation sources and plant operating schemes impact fuel characteristics, including minimum selling price (MSP) and lifecycle (LC) emissions. Considering the constraints on biomass availability, I further assess the environmental characteristics of biomass-efficient fuel production in a hybrid power- and biomass-to-liquid facility, using spatially resolved data for the United States (US).

Chapter 2

Methods

2.1 Pathway Scope

A review of the recent peer-reviewed academic literature on electrofuel technologies indicates that the most technically mature electrofuel production pathways, with near-term prospect for commercial-scale production, are those that use Fischer-Tropsch (FT) Synthesis [14]. FT synthesis is a well-established catalytic process that synthesizes carbon monoxide (CO) and hydrogen (H_2) into liquid hydrocarbon fuels, suitable for drop-in use in transportation applications. Four fuel production pathways using FT synthesis were identified for further analysis here: Biomass-to-Liquid (BtL); Power- and Biomass-to-Liquid (PBtL); and two Power-to-Liquid (PtL) pathways. The first PtL pathway includes both an electrolysis and reverse water gas shift (RWGS) unit, whereas the second uses a co-electrolysis unit. The process flow diagrams for each pathway are shown below in Figures 1-4.

The four pathways differ primarily in the sources of hydrogen and carbon used to generate syngas. The BtL pathway uses biomass as the source of both hydrogen and carbon. In contrast, the PtL pathways extract carbon from a gas stream, namely air or flue gases, while converting hydrogen from the electrolysis of water. The PBtL pathway is a hybrid of BtL and PBtL, which makes use of hydrogen extracted from water via electrolysis, and carbon from biomass gasification. The hydrogen and carbon sources for each pathway are summarized in Table 2.1.

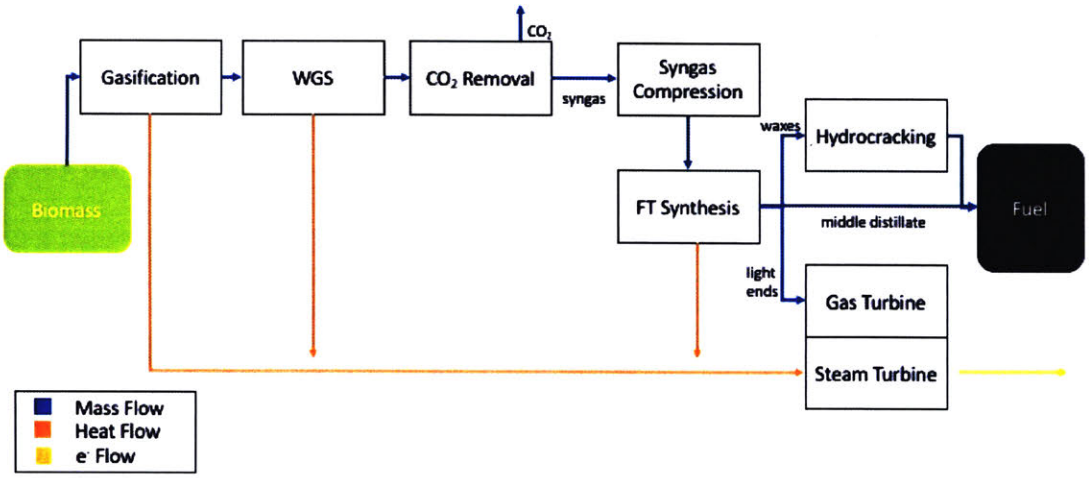

Figure 2-1: Biomass-to-Liquid (BtL) production pathway

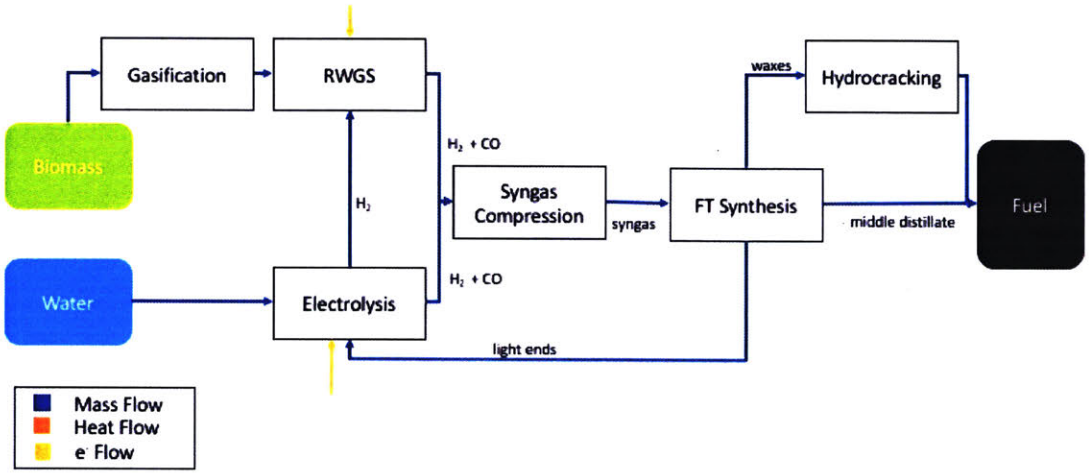

Figure 2-2: Power and Biomass-to-Liquid (PBtL) production pathway

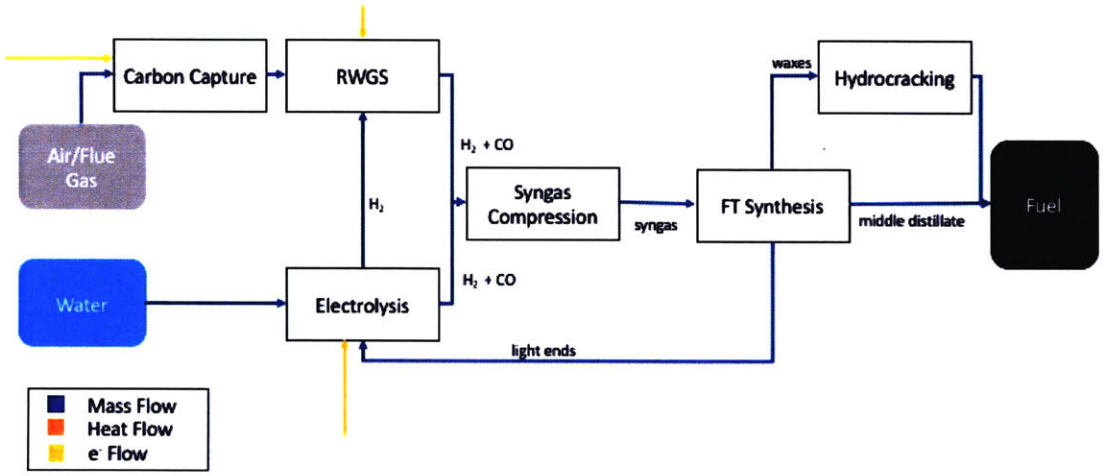

Figure 2-3: Two-Step Power-to-Liquid (PtL) production pathway using RWGS and electrolysis.

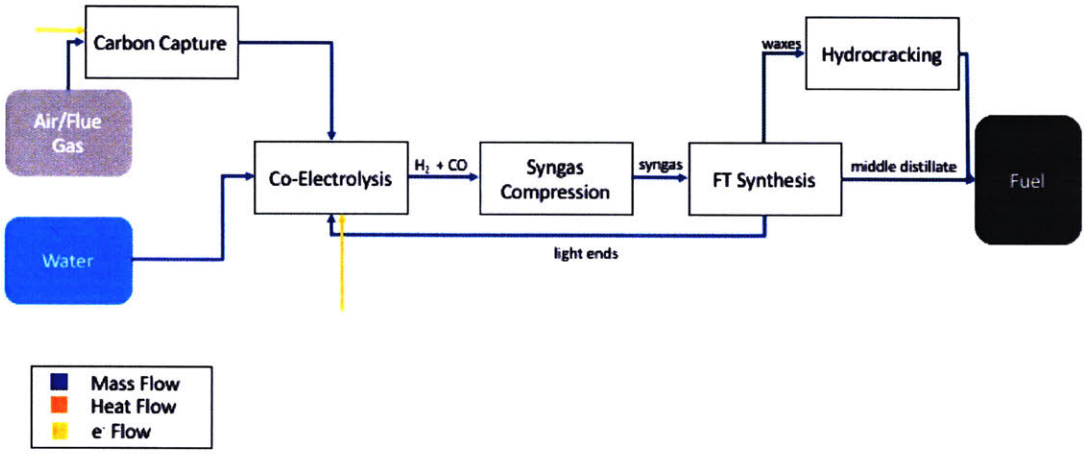

Figure 2-4: One-Step PtL production pathway using co-electrolysis.

Table 2.1: Hydrogen and carbon sources for each pathway

Pathway	Carbon Source	Hydrogen Source
BtL	Biomass	Biomass
PBtL	Biomass	Water
PtL Elec	Air/Flue Gas	Water
PtL CoElec	Air/Flue Gas	Water

Although BtL is not an electrofuel, it is included here to enable the comparison of results along a spectrum of FT fuels. Note that the BtL process co-produces electricity, while PtL and PBtL consume electricity. The biomass feedstock requirements of BtL are greater than for PBtL, and PtL does not require biomass feedstock input. By including this spectrum of technologies, we quantify the tradeoffs of using scarce biomass resources for alternative fuel production.

2.2 Process Unit Technologies

2.2.1 Biomass Feedstock & Gasification

In this analysis the biomass feedstock for the BtL and PBtL pathways is assumed to be switchgrass. Switchgrass is an attractive lignocellulosic feedstock because it is a native species to North America requiring minimal cultivation inputs, and it offers environmental benefits in terms of soil carbon sequestration [15] [16]. We note that future work could explore the impact of other biomass feedstocks on our results. The BtL pathway is assumed to use an air-steam gasifier resulting in excess heat that can be utilized for energy generation. In the PBtL pathway, oxygen from electrolysis is assumed to be fed into an oxy-steam gasifier that runs auto-thermally. The primary difference between these two gasification methods is the composition of the resulting syngas, with 34% greater carbon monoxide production by volume in the oxy-steam case [17].

2.2.2 Carbon Extraction from Gas Streams

For the PtL pathways, electricity is used to run a process that extracts carbon from a gas stream. This process can be used to extract carbon directly from the atmosphere or from flue gas emissions. In this analysis, it is primarily assumed that carbon is sourced directly from the air. There are currently two major technology options to directly extract carbon from the atmosphere that are commercially available. The first uses a solid sorbent to capture carbon, whereas the other uses an aqueous solution [18] [19]. Rather than select one of these two technologies, this analysis estimates the energy balance by adopting the theoretical framework proposed by House et al. (2011). This framework assumes a minimum energetic work required to extract carbon based on its concentration in the incoming gas stream. The total energy required is then calculated by varying 2nd law efficiencies, likely between 5-9% for direct air capture [20]. Equations 2.1 and 2.2 show how these values are used to calculate energy consumption,

$$E_{sp_{CO_2}} = \frac{W_{min}}{\eta} \tag{2.1}$$

$$E_{total} = \frac{m_{CO_2} E_{sp_{CO_2}}}{mw_{CO_2}} \tag{2.2}$$

where $E_{sp_{CO2}}$ is the specific energy per mole of CO_2 captured, W_{min} is the minimum work required to extract CO_2 based on its concentration in the gas stream, η is the second law efficiency, m_{CO2} is the mass of CO_2, mw_{CO_2} is the molecular weight of CO_2 in mass per mole and E_{total} is the total energy required for the process.

Using this approach, and assuming an 8% second law efficiency, yields an estimate of the required energy that is within 2% of the value reported by Keith et al. (2018) to produce a low pressure CO_2 stream with a free oxygen supply. All of the values used for calculation are included in Appendix A.

2.2.3 Fischer-Tropsch Synthesis

A low temperature cobalt catalyst reactor is assumed to be used for FT synthesis. To achieve optimal fuel production conditions in the reactor, this analysis assumes that the molecular ratio of hydrogen and carbon monoxide, H_2:CO, must be maintained at 2 [21] [22].

2.2.4 Hydrogen Sourcing

For all pathways, the source of hydrogen for the fuel is either electrolysis of water or biomass gasification. When biomass is used as a hydrogen source, the elemental components of fuel are released during the gasification process, with a resulting gas stream that has a H_2:CO ratio less than the required 2. Therefore, a water gas shift (WGS) process is required to adjust the ratio until it reaches this value. The WGS reaction formula is shown in Equation 2.4.

$$CO + H_2O \Leftrightarrow CO_2 + H_2 \quad \Delta H_R^0 = -41.2 \frac{kj}{mol} \tag{2.3}$$

The WGS reaction sacrifices CO to CO_2 emissions, in order to increase the quantity of hydrogen present, thereby decreasing the amount of carbon retained in the overall process. In pathways that extract hydrogen from water using electrolysis, no carbon monoxide needs to be sacrificed to achieve the correct syngas ratio, which enables higher overall carbon yields.

2.2.5 Solid Oxide Electrolysis

Many electrolysis methods exist, including Proton Exchange Membrane (PEM), alkaline, and high temperature Solid Oxide Electrolysis Cells (SOEC), also known as steam electrolysis. This analysis assumes SOECs are used, as they have the highest process efficiencies, and are expected to be commercially available in the near future [23] [24] [25]. In the 1-step process, a co-electrolysis SOEC is assumed to electro-chemically split H_2O and CO_2 into its component elements simultaneously.

Although the literature shows that this process has higher capital costs relative to SOECs that split only water, the benefits of co-electrolysis are in reducing the overall energy consumption and complexity for fuel production [26] [27].

2.2.6 Heat Integration & Electricity Generation

Excess heat from the exothermic processes in the BtL production pathway, WGS and FT synthesis, is assumed to be recovered for energy generation in a combined cycle gas and steam turbine. The heat is recovered in the steam turbine, while the combustion of light ends produced during synthesis, defined as hydrocarbons with less than 4 carbon atoms, drive the gas turbine. The electricity generated from the combined cycle is assumed to be sold as another value stream. For the other pathways, since the excess heat production is small relative to the energy inputs for fuel production, it is assumed that it is not economical to recycle the energy. Only the BtL process produces electricity as a co-product in this analysis.

2.2.7 Hydrocracking & Reformation

After FT Synthesis, the higher chain alkanes (C21+) are fed into the hydrocracker unit where they are cracked into smaller chains hydrocarbons suitable for transportation fuel. Small chain alkanes, (C<4) are fed into a gas turbine in the BtL case, or recycled in the electrolysis unit in the power based fuel pathways. The high temperature of the SOEC units allows the gas to be reformed into syngas [28]. This reformation is modeled as a steam methane reformation reaction using Equation 2.4.

$$CH_4 + H_2O \Leftrightarrow CO + 3H_2O \quad \Delta H_R^0 = +209\frac{kj}{mol} \tag{2.4}$$

The additional heat required and syngas produced is accounted for in the mass and energy balance model.

Table 2.2: RWGS process relevant values for stochastic modeling

Variable	Min	Max	Units	Description	Source	Details
Energy RWGS	41		kj/mol	Molar specific energy of reaction	Unde (2012)	Gold and Nickel Catalysts Tables 5-2 and 5-3
T	1023 15	1173 15	K	Temperature of reaction	Daza and Kunde (2016)	Unde (2012)
X_CO2	28	55	%	Conversion rate of reaction	Daza and Kunde (2016)	Looked at CO selectivities of 100

2.3 Stochastic Mass & Energy Balance Models

Mass and energy balance models were built to characterize each of the pathways of interest. Each process step in a pathway was parameterized by its relevant variables to quantify the associated energy and mass flows, and values from literature are used to estimate the expected performance of each process. These values are represented stochastically using a uniform distribution between the maximum and minimum values reported in the literature for each variable, in order to quantify uncertainty in overall process mass and energy balances. Table 2.3 gives an example of the maximum and minimum values used for a single process, RWGS, and all of the values used in the model are included in Appendix A.

The results of the mass and energy model are used as the basis for the life cycle and techno-economic assessments. In addition, the energy and carbon efficiencies calculated directly from the mass and energy balances are useful metrics of comparison between the pathways assessed here.

For example, XtL efficiency is defined as the energy in the transportation fuel divided by the total energy input into the system through electricity or biomass, as shown in Equation 2.5

$$\eta_{\mathrm{XtL}} = \frac{\mathrm{m_{pr}LHV_{pr}}}{\mathrm{m_{biomass}} + \mathrm{LHV_{biomass}} + \mathrm{E_{elec}}} \tag{2.5}$$

where η_{XtL} is overall energy efficiency of the plant; $\mathrm{m_{pr}}$ and $\mathrm{m_{biomass}}$ are masses of product and biomass, respectively; $\mathrm{LHV_{pr}}$ and $\mathrm{LHV_{biomass}}$ are the lower heating values of the product and biomass, respectively; and $\mathrm{E_{elec}}$ is the energy input as electricity.

In contrast, carbon efficiency is defined as the carbon in the transportation fuel product divided by the carbon input into the system from direct air extraction, flue gas extraction, or biomass gasification, as shown in Equation 2.6:

Table 2.3: Example mass and energy balance outputs for the PBtL pathway

PBtL M&E Balance			
Mass In	Biomass	1000	kg
Mass In	H2	3.25	kg
Mass In	H2O	1475.84	kg
Mass Out	Fuel	481.78	kg
Mass Out	Waxes	5.85	kg
Mass Out	O2	525.5	kg
Mass Out	Gasoline	228.15	kg
Mass Out	Diesel	91.05	kg
Energy	Heat	-1660.69	MJ
Energy	Electricity	17318.63	MJ
Efficiency	XtL	0.6	[-]
Efficiency	Overall	0.6	[-]
Efficiency	Carbon	0.82	[-]

$$\eta_C = \frac{n_{c_{pr}}}{n_{c_{biomass}} + n_{c_{CO2stream}}} \tag{2.6}$$

where η_C is overall plant carbon efficiency; $n_{c_{pr}}$, $n_{c_{CO2stream}}$ and $n_{c_{biomass}}$ are the number of carbon atoms in the biomass, input CO_2 stream and products, respectively. The carbon content values for the biomass and products, diesel and gasoline, are sourced from the Greenhouse Gases, Regulated Emissions, and Energy Use in Transportation (GREET) model, a commonly used life cycle emissions inventory [8] [29]. All values are listed in Appendices A and B.

The energy and carbon efficiency results for the fuel production pathways are shown in Figures 2-5 and 2-6. For PtL fuels, a 10% increase in energy efficiency can be achieved by sourcing carbon from flue gas rather than directly from air. However, this pathway is not considered subsequently in this report due to its relatively poor life cycle emissions performance [30].

An example of the mass and energy outputs from the models is shown in Table 2.3. Although hydrogen shows up as a net input, it is assumed that this hydrogen, required for the hydrocracking unit, is supplied by increasing the output of the electrolysis unit. This additional energy consumption, a 0.3% increase, is considered negligible

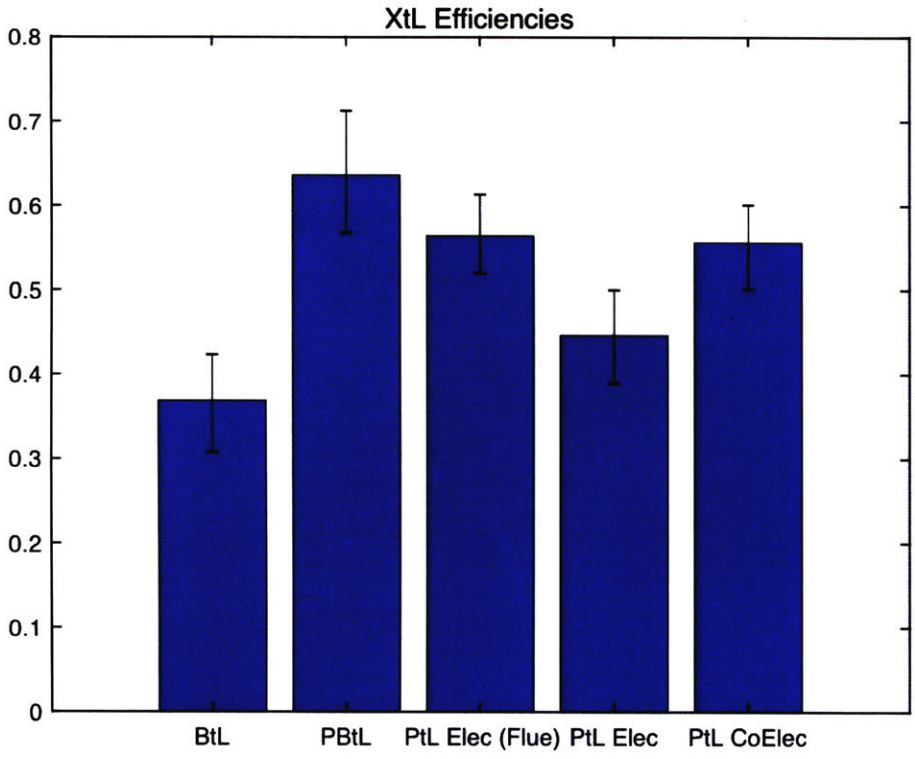

Figure 2-5: PBtL has the highest energetic efficiency of all pathways. Co-electrolysis improves the energy efficiency of PtL fuel production.

2.4 Life Cycle Analysis

The life cycle analysis (LCA) is carried out using the outputs from the mass and energy balance models. A well-to-wheel/wake analysis is considered, using a system boundary extending from biomass/feedstock cultivation and collection, transportation, feedstock-to-fuel conversion, and ultimately the combustion of the transportation fuel. Figure 2-7 shows the system boundary used.

Greenhouse gas (GHG) emissions that occur within the system boundary are accounted for including fuel production emissions, fuel transportation, and fuel combustion. Emissions values for each material input are sourced from GREET. To determine the emissions from electricity generation, emissions values are taken from a dataset based on the NREL Renewable Futures 2012 Study [31]. Material flows that account for less than 3% of the overall emissions are considered negligible for the purposes of

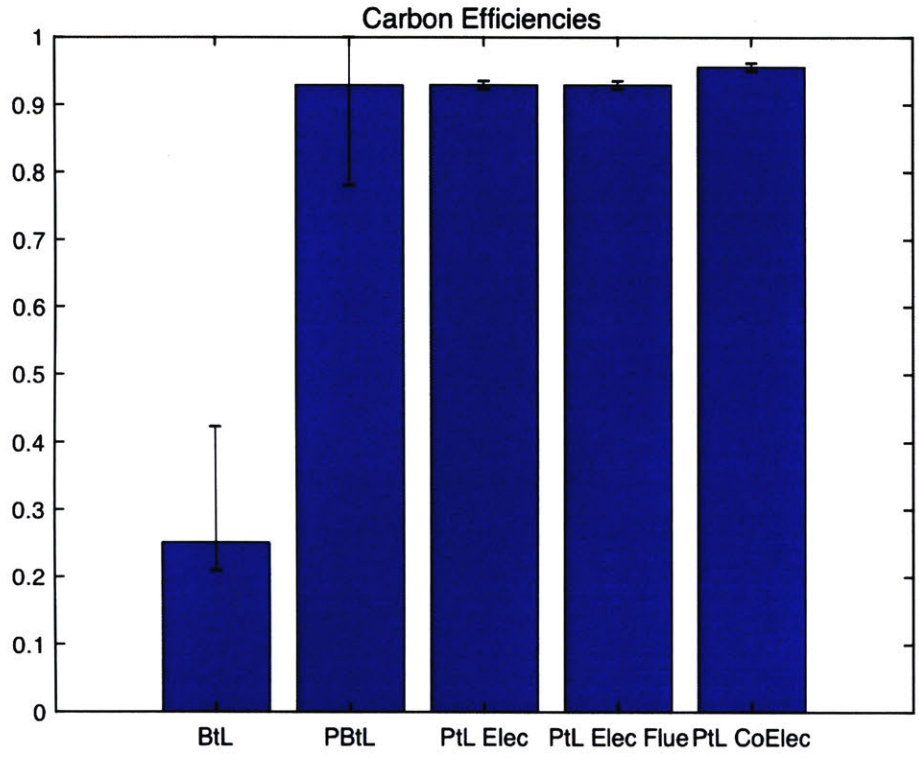

Figure 2-6: The PtL and PBtL pathways have high carbon efficiencies relative to conventional BtL pathways using gasification and Fischer-Tropsch synthesis.

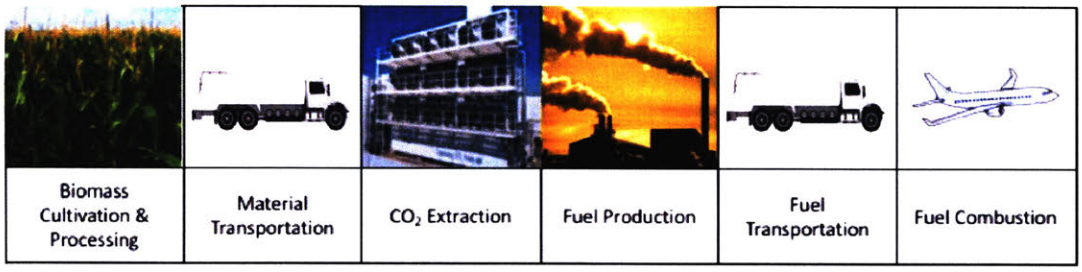

Figure 2-7: Fuel production processes considered in the LCA

this analysis. This includes the emissions associated with FT replacement catalyst materials and DAC process waste chemicals. In the PtL pathways, carbon dioxide is assumed to be extracted directly from air and then re-released during combustion, thus neither adding nor subtracting from the carbon balance of the atmosphere. An energy allocation method is used to determine the emissions associated with each useful product based on its lower heating value. The fuel products considered include

diesel and jet range middle distillate fuels, as well as co-produced electricity in the case of the BtL pathway.

2.5 Techno-economic Assessment

The techno-economic assessment (TEA) uses the results from the mass and energy balance model to estimate the costs of fuel production. Fuel production capacities of approximately 11 t/hr and 2.9 t/hr for the power based pathways (PBtL, PtL Electrolysis + RWGS and PtL Co-electrolysis) and BtL were chosen, respectively, to allow for direct comparison with Albrecht et al. (2018). Methods for estimating capital expenditures (CAPEX) and operating expenditures (OPEX) were adapted from Albrecht et al. (2018) to quantify fuel production costs.

CAPEX is estimated by calculating the equipment costs and fixed capital investment (FCI). The equipment costs are estimated based on the nominal process unit cost and a scaling factor, as shown in Equation 2.7,

$$\mathrm{EC}_i = \mathrm{EC}_{\mathrm{ref}_i} \left(\frac{\mathrm{S}_i}{\mathrm{S}_{\mathrm{ref}_i}}\right)^d \tag{2.7}$$

where EC_i is the equipment cost for the modeled process unit, $\mathrm{EC}_{\mathrm{ref}}$ is the reference equipment cost at nominal capacity, $\mathrm{S}_{\mathrm{ref}}$ is the reference capacity, S_i is the modeled capacity, and d is the appropriate scaling factor. Appendix C includes the values used for each process.

The initial equipment cost values are then multiplied by direct and indirect factors and summed to determine the FCI. FCI is calculated using Equation 2.8,

$$\mathrm{FCI} = \sum_{i=1}^{m} \mathrm{EC}_i \left(1 + \sum_{j=1}^{10} \mathrm{F}_{i,j}\right) \left(1 + \sum_{j=11}^{12} \mathrm{F}_{i,j}\right) \tag{2.8}$$

where $\mathrm{F}_{i,j}$ is the indirect factor that corresponds to the value for j in Table 2.5, to be accounted for in the pricing of process unit, i. When calculating the costs for the electrolysis and co-electrolysis units, only equipment installation, instrumentation and control, yard improvements, legal expenses, contractor's fee and contingency factors

Table 2.4: Indirect Cost item list from Albrecht et al. (2018)

Indirect Cost items	j	Typical Value
Total direct plant costs (D)		
Equipment installation	1	0.47
Instrumentation and control	2	0.36
Piping (installed)	3	0.68
Electrical (installed)	4	0.11
Buildings including services	5	0.18
Yard Improvements	6	0.1
Service Facilities (installed)	7	0.55
Total Indirect plant costs (I)		
Engineering and supervision	8	0.33
Construction Expenses	9	0.42
Legal Expenses	10	0.04
As function of (D+I)		
Contractor's Fee	11	0.05
Contingency	12	0.1

are considered in order to be in agreement with literature estimates of equipment cost. An example of the output capital costs and FCI is shown in Table 2.5.

The OPEX cost estimation sums the direct material and energy costs, indirect material costs and labor costs, in line with the approach used by Albrecht et al. (2018). For OPEX calculations, the electricity and biomass costs are assumed to be fixed over the lifetime of the plant, with the electricity cost specified in the analysis scenario and the biomass cost used in Albrecht et al. (2018). All of the values used

Table 2.5: Equipment Capital Costs for a PtL Electrolysis + RWGS plant factoring in direct and indirect costs.

Process	Capacity	Units	Equipment Cost ($MM 2016)
CO2 Capture	1088	tCO_2/day	1047
RWGS	1088	tCO_2/day	8
Electrolysis	270.5	MW	483
Compress	3264.6	kW	14
FT Synth	141.4	m^3	73
Hydrocracking	0.2	kg/s	15
Total FCI			1650

are included in Appendix C.

The CAPEX and OPEX values are then used to evaluate the minimum selling price (MSP) using a Discounted-Cash Flow Rate of Return (DCFROR) model, as described in Pearlson et al. 2013 and Bann et al. 2017 [32] [33]. This model calculates a Net Present Value (NPV) for fuel production by calculating the net cash flows in and out of the plant over its lifetime. The model then iterates on a fuel price until a NPV of zero is achieved. Positive cash flows include the selling of jet and diesel fuels, and electricity, on the market. The power price is specified deterministically in each analysis scenario. The biomass feedstock is assumed at a fixed cost of $122/tonne [2]. Oxygen is not assumed to be a valuable co-product in this analysis. Financial assumptions for each pathway include a 20-year plant lifetime with 20% equity financing and a 10-year loan with 10% interest. Each plant was assumed to operate at a 95% capacity factor, or 350 days per year. All financial assumptions and cost values are included in Appendix C.

Chapter 3

Results and Discussion

The results for the analysis are discussed here. The initial results are evaluated using parameterized electricity characteristics, specifically with independently varying life cycle emissions and cost. The characteristics significantly depend on the source of power generation. Therefore, I next consider cases in which there is dedicated on-site generation of renewable electricity, in order to guarantee lower life cycle GHG emitting electrofuel. This assumes an electricity generation facility is built at a scale sufficient to entirely offset the power requirements of electrofuel production. The results indicate that the hybrid power- and biomass-to-liquids (PBtL) pathway utilizing renewable power may represent a promising option for electrofuel production in terms of life cycle emissions reductions and low minimum selling price. I further characterize the PBtL pathway by combining spatially-resolved data on biomass cultivation, electricity generation, and cost-optimized solar-hydrogen production in the United States (US).

3.1 Parameterized Electricity Characteristics

3.1.1 Life Cycle Analysis Results

The results of the LCA show that power based fuel production is highly sensitive to the life cycle emissions associated with electricity generation. This is even more apparent

for pathways that require larger quantities of electricity, such as the PtL Electrolysis + RWGS pathway, which requires an input electrical energy to output fuel energy ratio of 2.4, compared to 1.8 and 0.8 for PtL co-electrolysis and the PBtL pathways, respectively. The life cycle GHG emissions results are shown in Figure 3-1. The sensitivity of a fuel pathway's emissions to the emissions from electricity generation can be determined by the gradient of the slopes in the figure. The BtL production pathway has constant life cycle GHG emissions, since no external electricity is required for fuel production.

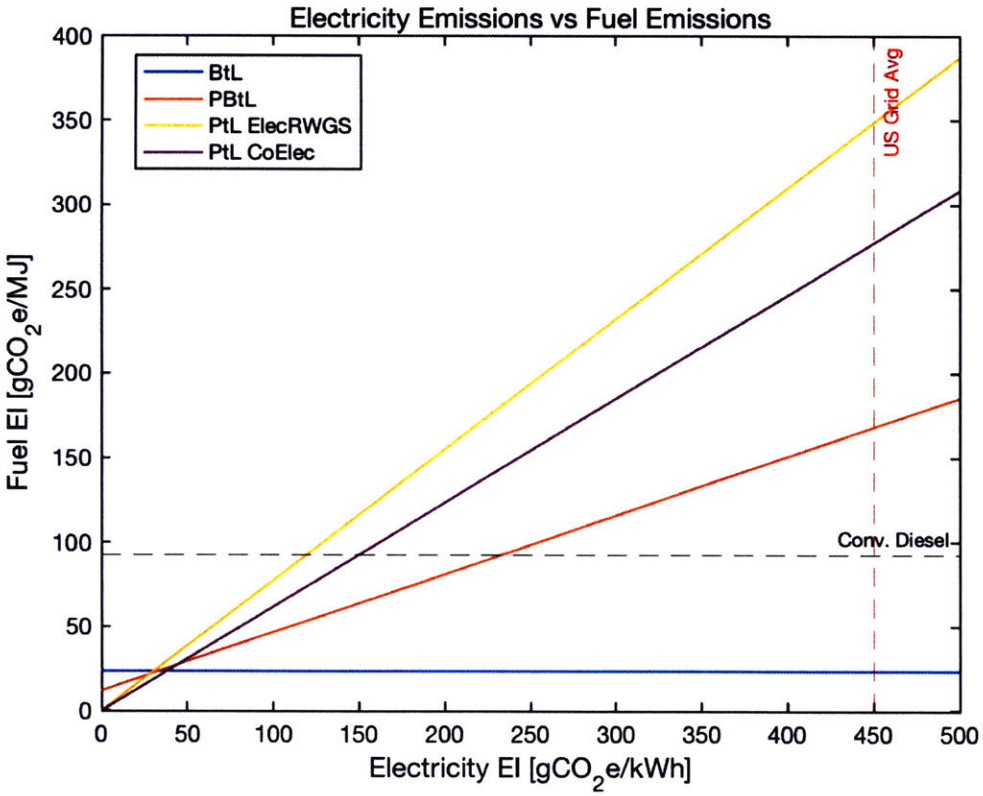

Figure 3-1: Electricity emissions strongly determine the GHG emissions of electrofuels. Production pathways that use more electricity are more sensitive to this value. PtL pathways using low EI energy have the greatest emission reduction potential.

If the current average U.S. grid electricity generation emissions index of 450 gCO_2e/kWh is assumed, the calculated life cycle GHG emissions from electrofuels are between 1.5-3.5 times greater than conventional diesel [34] [35]. However, using renewable sources can reduce the life cycle emissions from fuel pathways down by 93%.

Table 3.1: Breakeven electricity emission index values for electrofuel production pathways

Pathway	Breakeven Grid EI [gCO2e/kWh]
PBtL	225
PtL ElecRWGS	125
PtL CoElec	150

For example, assuming wind powered electricity generation, with life cycle emissions of 11 gCO_2e/kWh, the PtL co-electrolysis pathway yields the greatest emissions reductions with life cycle emissions of 6 gCO_2e/MJ. For electricity grid scenarios where electricity comes from a mix of non-renewable and renewable sources, the 'breakeven' point indicates the grid electricity emissions index at which point the climate impact of the electrofuel in question is equivalent to petroleum-derived diesel. The breakeven point for each fuel production pathway is shown in Table 3.1.1.

The results shown in Table 3.1.1 demonstrate that electrofuel production pathways with a lower breakeven point require grid energy composed of more renewable electricity sources to achieve parity with petroleum-derived diesel. Electric grids with a high composition of renewables have lower life cycle GHG emissions, and maximize the potential environmental benefit of electrofuels.

3.1.2 Techno-economic Assessment Results

Similar to the LCA results, the TEA results demonstrate that the conclusions of this study are highly sensitive to the source of electricity generation. In particular, the MSP of the fuel has a linear relationship with the assumed cost of electrical power. Again, the electrofuel production pathways that use more electricity are more sensitive to this cost, as shown in Figure 3-2, by having steeper slopes.

Unlike the PtL and PBtL pathways, the MSP of BtL is inversely related to electricity cost. Higher electricity prices generate more income in BtL facilities from the sale of co-produced electricity, thereby subsidizing the cost of fuel. The results from this analysis show that none of the assessed electrofuel production pathways are less expensive than conventional diesel on a per liter basis. The PtL pathways have the

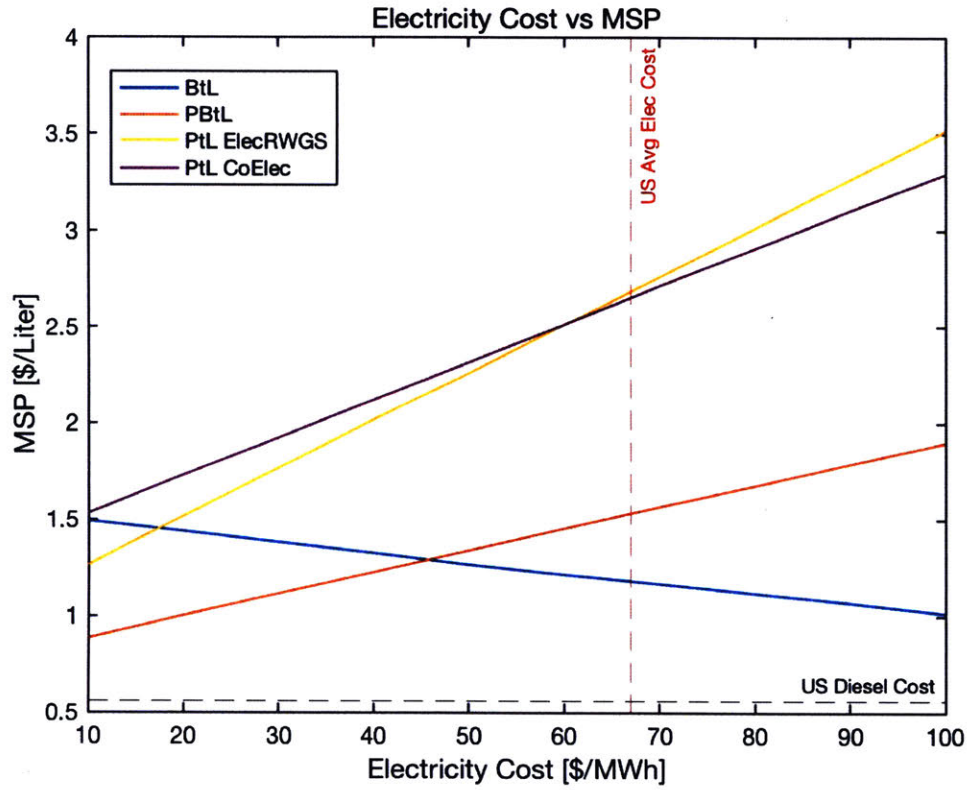

Figure 3-2: Electricity cost strongly determines the overall production cost of electrofuels. Although production pathways that use more electricity are more sensitive to this value, capital costs also account for major cost differences between pathways.

greatest MSPs, and are from 2.5-7 times more expensive than conventional fuel on a per liter basis.

3.2 Dedicated Renewable Power Generation

Previous analyses were conducted under a parameterized electricity grid, where the electricity cost and emissions were varied independently. In practice, electricity cost and GHG emissions are closely related based on the generation method. To account for this, I considered additional scenarios in which dedicated electricity generation capacity is built on, or near, the site of the electrofuel plant. This is consistent with strategies being considered by companies seeking to commercialize technologies similar to those considered in this study. These firms enter into power purchase

agreements with electricity generators, which are typically located in proximity to the fuel production facilities, in order to ensure that the power used for electrofuel production is advantageous from a production cost and environmental perspective [36].

The sizing of the electricity generation units is determined based on the net energy required to run the fuel generation process for 24 hours. Using capacity factor values, this is translated into a nominal power capacity using Equation 3.1,

$$P_{gen} = \frac{E_{plant}}{CF\,24hrs} \tag{3.1}$$

where P_{gen} is the power capacity, E_{plant} is the energy consumed by the production plant in 24 hours, and CF is the capacity factor of the generation unit. Capital costs are based on the power capacity. The capacity factor and capital cost values were taken from Tidball et al. (2010) and along with the assumed emissions indices from NREL (2012) are included in Appendix D [37].

The findings (Figure 3-3) demonstrate that wind and nuclear energy generation appear to be the most promising power sources when considering the MSP and life cycle GHG emissions of electrofuel pathways. These sources of electricity generation perform best in terms of life cycle GHG emissions and MSP, as shown by their positions nearest the bottom left corner in Figure 3-3, relative to other generation sources for a given pathway.

The results in Figure 3-3 highlight the tradeoffs between the production cost and emissions reductions of electrofuel pathways. In general, the fuel production pathways that achieve the greatest life cycle GHG emissions reductions come at a greater cost premium. A comparison of the MSP and life cycle GHG emissions of each pathway is given in Table 3.2. The average US grid electricity is assumed to emit 450 gCO_2e/kWh at a price of \$67.30/MWh, and dedicated wind power is assumed to emit 11 gCO_2e/kWh at a capital cost of 1031 \$/kW [34] [37].

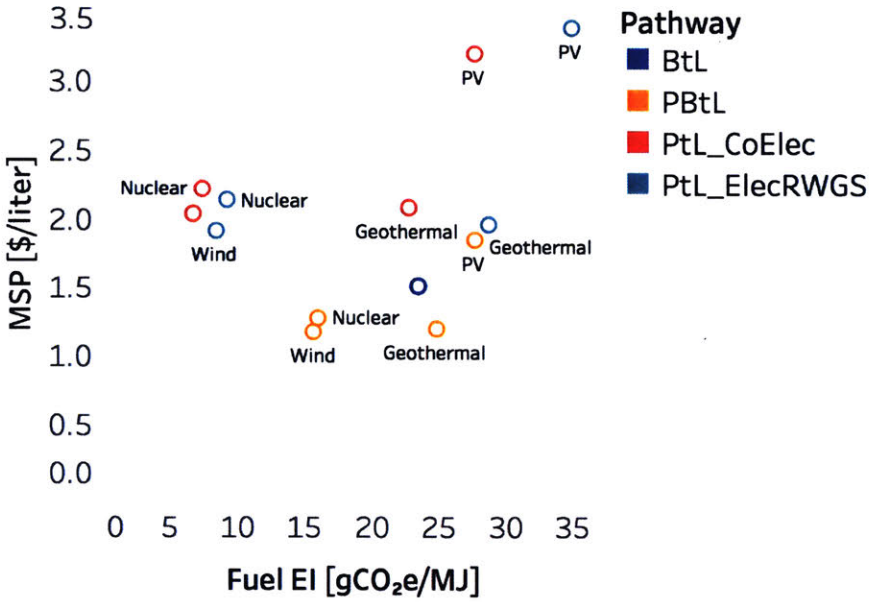

Figure 3-3: Wind and nuclear powered electrofuel pathways perform best in the tradeoff between net present cost and greenhouse gas emissions of electrofuels

Table 3.2: Life cycle emissions and MSP for electrofuel production pathways

Pathway	Average US grid electricity		Dedicated wind electricity	
	LCA Results (gCO_2e/MJ)	MSP ($/L)	LCA Results (gCO_2e/MJ)	MSP ($/L)
Diesel	92	0.56	92	0.56
BtL	23	1.18	23	1.18
PBtL	168	1.53	16	1.18
PtL Elec	349	2.7	8	1.92
PtL CoElec	277	2.66	7	2.04

3.3 Solar-Hydrogen Production for Hybrid Power and Biomass to Liquid Electrofuel Plants

In the power-derived fuel pathways considered in this analysis, electrolysis for hydrogen production is the largest single contributor of demand for power and capital costs, equal to 90% of electricity consumption and 40% of total capital cost in the PBtL pathway. Therefore, a more detailed investigation of options to mitigate emissions and costs associated with hydrogen production is undertaken here. Specifically, the PBtL pathway in considered, as it offers the potential for life cycle emissions reduction approaching those of the PtL pathways, at a significantly smaller production cost

premium. The previous methodology has limitations in the insights it can yield for this configuration as it does not account for the storage required due to renewable power generation intermittency, nor does it adequately capture the regional differences in generation potential. Therefore, I propose a self-contained system to narrow down the characteristics of the technology configuration.

In particular, I assess the case of dedicated solar powered hydrogen generation for electrofuel production. Similar to using dedicated renewable energy generation, this strategy helps to reduce the dependence of fuel life cycle emissions on the composition of the power grid, by reducing demand for input electricity. The performance of the PBtL pathway is further characterized by combining spatially-resolved data on biomass cultivation, electricity generation, and cost-optimized solar-hydrogen production in the United States (US).

An adapted version of the PBtL plant, shown in 3-4, is evaluated using existing unit process unit models and similar LCA and TEA analysis methods. One difference is the gasification process is switched to air steam gasification since a free oxygen supply is no longer assumed to be available. Another difference is that light ends ($C<4$) produced during Fischer-Tropsch synthesis can no longer be recycled in the electrolysis unit. The plant therefore also co-produces synthetic natural gas as an economically valuable output. Life cycle analysis is carried out on an energy allocation basis, with the synthetic natural gas product's energetic content included.

Biomass data is sourced from the US DOE Billion Ton Study 2016, with availability and cost data given on a per county basis for 2030 [38]. I use zonal spatial analysis to fit latitudinal and longitudinal H_2 production cost data from Mallapragada et al 2019 into average values for each biomass-producing county [39]. The national electricity grid composition of generation sources is estimated using projections from EIA Annual Energy Outlook 2018, and life cycle emissions factor for the grid is derived with values from the NREL Renewable Futures Study [40] [31]. State-level emissions data are from the US Environmental Protection Agency eGrid summary tables 2016 to normalize each state's emissions relative to the national average [34]. This ratio is assumed to remain constant into the future, and is multiplied by the national grid

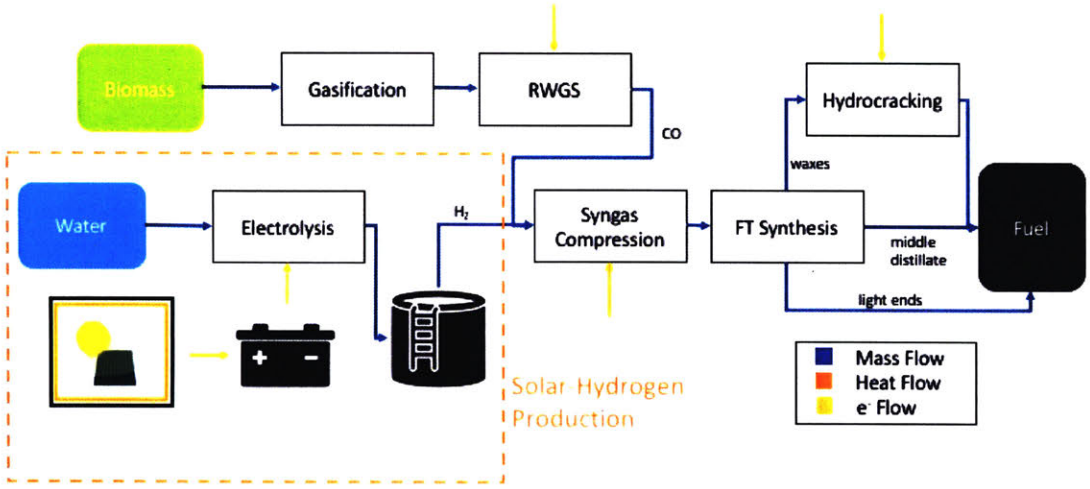

Figure 3-4: Solar-Hydrogen supplied PBtL process flow diagrams. Differs slightly from previously modeled PBtL pathway

average to determine the state's , and all of that state's counties' , electricity emissions factors. A similar method is done using EIA Annual Energy Outlook information on state-level industrial electricity costs to project future county-level price information. The full data re-gridding procedure and its relationship with the the mass and energy balance model is shown in Figure 3-5.

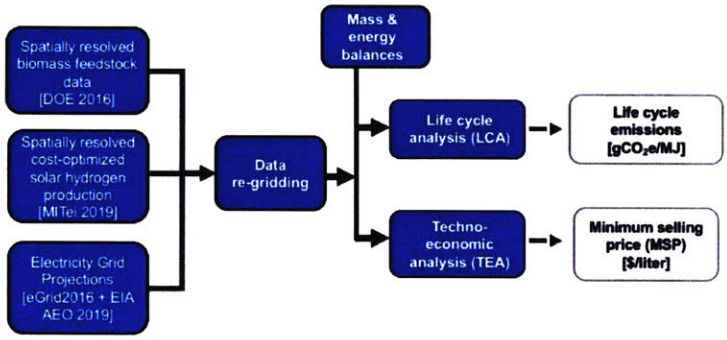

Figure 3-5: Spatially-Resolved Datasets from three main sources are regridded to supply county-level information for analysis

This data is used to select the lowest cost feedstock available in each county in

the US, shown in Figure 3-6. Many counties in the western US have no feedstock availability and are therefore left uncolored. Corn stover, switchgrass and willow were chosen as feedstocks to be representative of major lignocellulosic biomass types. These types include herbaceous biomass, agricultural residues and short-rotation woody crops. I expect that feedstocks of similar type such as poplar and miscanthus, will yield results close to their chosen representative.

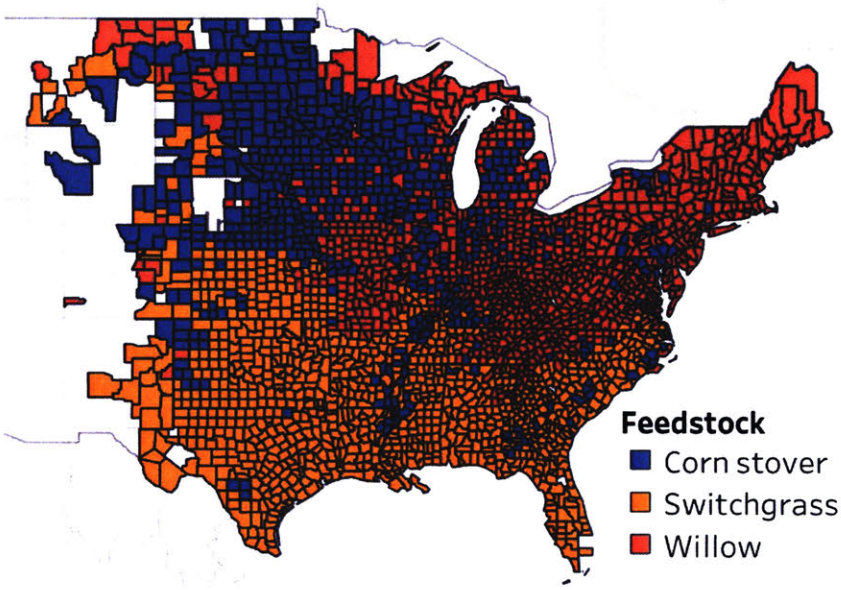

Figure 3-6: Lowest cost feedstock with availability in each county in 2030 from the US Department of Energy Billion Ton 2016 report.

Analyzing the production pathway performance given the feedstock selection and costs results in county-level results for MSP and life cycle emissions of PBtL using solar-hydrogen as shown in Figures 3-7 and 3-8. Assuming petroleum diesel costs of \$0.56 per liter, and life cycle emissions of 92 gCO_2e per megajoule, Figure 3-9 also shows the estimated private cost of CO_2e emissions abatement via this technology pathway.

The results suggest that for this technology configuration, solar insolation is the determining factor for MSP, with values between from \$2.10-3.81 per liter. The lowest MSP values occur in areas receiving the greatest solar insolation, consequently that produce hydrogen at the lowest cost. In contrast, feedstock selection is the most important determinant of life cycle emissions, with values ranging from 15.4-27.1

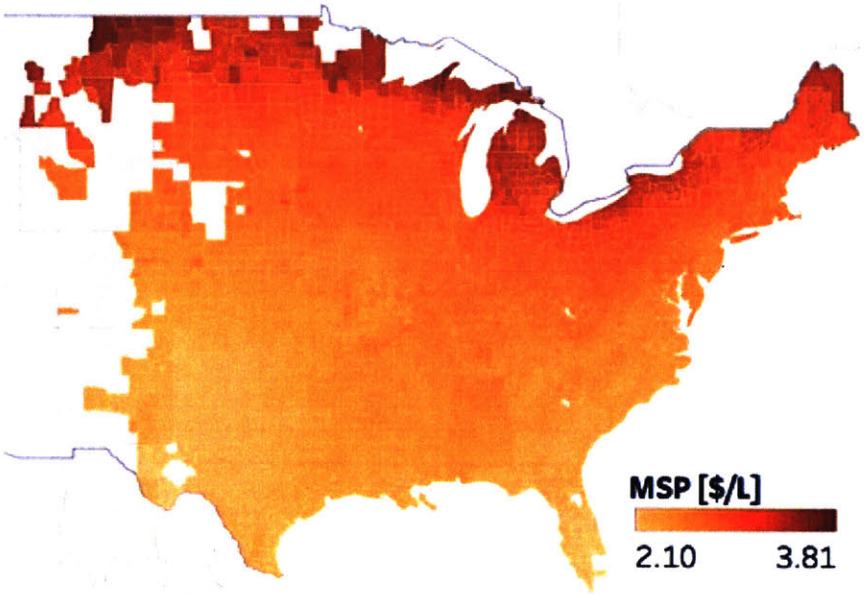

Figure 3-7: Minimum selling price values for PBtL electrofuel production

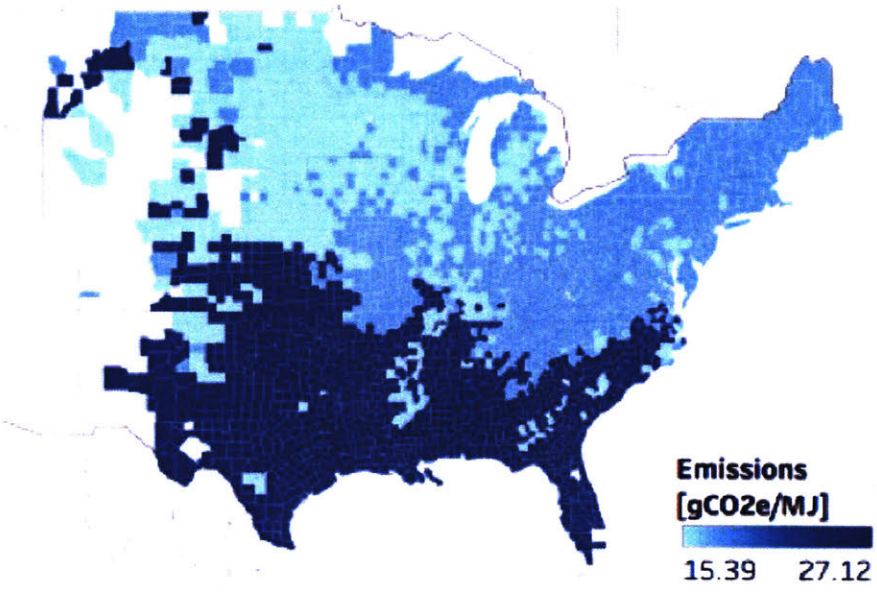

Figure 3-8: Life cycle emissions values for PBtL electrofuel production

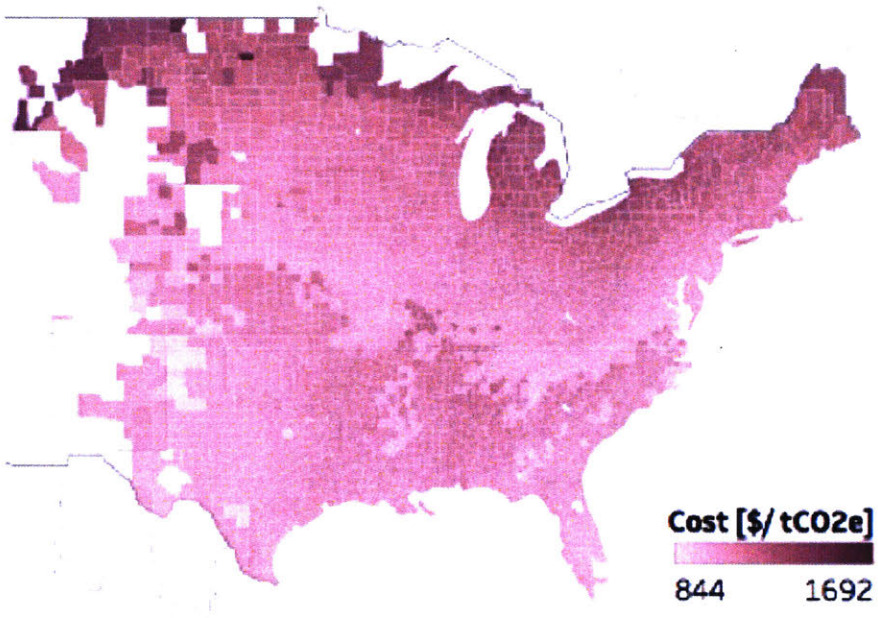

Figure 3-9: Private abatement costs for PBtL electrofuel production

gCO_2e/MJ. This can be observed by comparison of the patterns in Figures ?? and 3-8. Feedstocks have different emission characteristics due to differences in production inputs such as nitrogen fertilizer, as well as varying harvesting and transportation methods [16]. As a point of reference, biofuels produced from switchgrass using advanced fermentation methods yield a baseline LC emission value of 37.4 gCO_2e/MJ and a minimum selling price \$2.30 per liter of middle distillate [8].

Private abatement costs, the cost of avoiding a ton of CO_2e emissions by using PBtL in place of petroleum fuels, ranges from \$844-1692/tonne. The relative uniformity of abatement costs highlights that in the US, the location of potentially low emissions biomass feedstocks (such as agricultural residues and short-rotation woody crops), is not complementary to areas of high solar insolation, yielding low-cost solar-hydrogen production (such as the Southwest). Additionally, these values are high relative to abatement cost estimates for biodiesel between \$150-250 per tonne, but within the range of abatement cost estimates for photovoltaic subsidies between \$140-2100 per ton [41].

Chapter 4

Conclusion and Future Work

My analysis demonstrates that the life cycle emissions and production costs of electrofuels are highly dependent on the emissions and costs associated with input power production, which is largely a function of the type of generation. The PtL co-electrolysis pathway can reach life cycle GHG emissions reduction of up to 93% relative to petroleum diesel when using dedicated wind power, but comes at a production cost of $2.04/liter, approximately 3.6 times current petroleum diesel prices. At US average electricity prices, BtL is the lowest cost pathway examined at $1.18/liter, or a production cost 2 times that of petroleum diesel and life cycle GHG emissions reductions of 75%. When produced using dedicated wind power, the hybrid PBtL pathway yields an 83% emissions reduction relative to petroleum-derived diesel at a cost premium similar to BtL produced fuel. We find that wind and nuclear are the most advantageous power sources for electrofuel production, considering trade-offs between production costs and GHG emissions reductions.

However, given the intermittent nature of renewable power generation, it is impossible to guarantee that renewable electricity fed into the grid is indeed used to power the process of interest. Therefore, we consider the production of cost optimized solar-hydrogen as a means to ensure a renewable power input to PBtL electrofuel production. Under this technology configuration, we find MSP values between $2.10-3.81/L and lifecycle emissions between 15-27 gCO_2e/MJ, depending on location in the contiguous US. We find that the locations for low-cost hydrogen and low-emissions

biomass feedstocks are not coincident, therefore there are limited opportunities to minimize the private cost of CO_2e emissions abatement using this technology pathway. Future work in this area could consider additional plant integration with renewable power generation. In particular, wind power may present an opportunity to perform well due to its low-cost and low-emitting electricity generation and its availability near areas with low emitting corn stover production.

Appendix A

Mass and Energy Balance Model Process Variables and Sources

Table A.1: Common Variables

Molar Masses	Value	Value 2	Unit	Source
H2	0.002		kg/mol	
CO	0.028		kg/mol	
CO2	0.044		kg/mol	
CH4	0.016		kg/mol	
H2O	0.018		kg/mol	
O2	0.0319988		kg/mol	
mw_syngas	0.032		kg/mol	
Ideal Gas Constants				
R_univ	8.314		J/mol-K	
P_atm	101325		Pa	
T_std	288.15		K	
Specific Energy				
LHV_fuel	43		MJ/kg	
LHV_biomass	17.4	20.1	MJ/kg	GREET 2017
LHV of Components				
H2	120		MJ/kg	
CO	10.1			
CO2	0			
CH4	50			
Ethylene	47.2			
Nitrogen	0			
Assumed Chemical Compositions				
Fuel	C(12.5)H(27)			
biomass_c_comp	49.9	50.6	wt%	GREET 2017

Table A.2: Compressor

Variable	Min	Max	Units	Description	Source	
efficiency	70	85	%	Isentropic Efficiency for compressor	plant design and economics for chemical engineers	
Z	0.9	1.1	N/A	Compression Factor		
n	1.05		N/A	Heat Capacity Ratio	Carbon Engineering	Greet 2017
Specific Energy CO2	360		kJ/kg	CO2 CCS Compression Energy	GREET 2017	

Table A.3: Air Steam Gasification

Variable	Min	Max	Units	Description	Source
Gas Yield	2.23	2.34	Nm^3 Syngas/kg Biomass		Lv et al 2003
Steam Ratio	1.35	2.7	kg/kg	Ratio of mass of steam required per kg Biomass in reaction	Lv et al 2003
CGE	52.5	71.5	%	Cold gas efficiency of the process	Meng et al 2010
Tar yield	5.7	12.4	g/Nm^3	Tar yield per Nm^3 of syngas produced	Meng et al 2010
Char yield			kg/kg		
Syngas Volume %					
H_2	52.4		% element / Nm^3 Syngas	volume fraction of the element in the overall syngas mixture	Unruh et al 2010
CO	28.7		% element / Nm^3 Syngas	volume fraction of the element in the overall syngas mixture	Unruh et al 2010
CO_2	16.8		% element / Nm^3 Syngas	volume fraction of the element in the overall syngas mixture	Unruh et al 2010
CH_4	2.1		% element / Nm^3 Syngas	volume fraction of the element in the overall syngas mixture	Unruh et al 2010

Table A.4: Oxy-Steam Gasification

Variable	Min	Max	Units	Description	Source
Gas Yield	1.24	1.62	Nm^3 Syngas/kg Biomass		Meng et al 2010
Steam Ratio	1.04	1.42	kg/kg	Ratio of mass of steam required per kg Biomass in reaction	Meng et al 2010
Oxy Ratio	0.2	0.5	kg/kg	Ratio of mass of oxygen required per kg of Biomass	Meng et al 2010
CGE	52.5	71.5	%	Cold gas efficiency of the process	Meng et al 2010
Tar yield	5.7	12.4	g/Nm^3	Tar yield per Nm^3 of syngas produced	Meng et al 2010
Char yield			kg/kg		
Syngas Volume %					
H2	31		% element / Nm^3 Syngas	volume fraction of the element in the overall syngas mixture	Unruh et al 2010
CO	38.6		% element / Nm^3 Syngas	volume fraction of the element in the overall syngas mixture	Unruh et al 2010
CO2	27.2		% element / Nm^3 Syngas	volume fraction of the element in the overall syngas mixture	Unruh et al 2010
CH4	3.1		% element / Nm^3 Syngas	volume fraction of the element in the overall syngas mixture	Unruh et al 2010

Table A.5: Water Gas Shift

Variable	Value	Units	Description	Source
Energy WGS	-47.4	KJ/mol	Molar specific energy of reaction	Smith et Al 2010
H2 ratio	2	%molH2/%molCO	Molar ratio of H2 to CO	0
Catalyst Type	Cu-ZnO- Al2O3 (EX-2248)Sud Chemie	N/A	The catalyst referenced in Smith et al	Smith et al referencing Choi and Stenger (2003)

Table A.6: Reverse Water Gas Shift

Variable	Min	Max	Units	Description	Source 1	Source 2
Energy RWGS	41		KJ/mol	Molar specific energy of reaction	Unde 2012	Gold and Nickel Catalysts: Tables 5-2 and 5-3
T	1023.15	1173.15	K	Temperature of Reaction	Daza & Kuhn 2016	Unde 2012
X CO2	28	55	%	Conversion Rate of Reaction	Daza & Kuhn 2016	Looked at CO selectivities of 100

Table A.7: Steam Methane Reformation

Variable	Min	Max	Units	Description	Source
T	1023	1073	K	Temperature of reaction	SMR Factsheet
Energy of reaction	206		Kj/mol	Molar specific energy of reaction	Tabrizi et al 2015
Efficiency of reaction	65	75	%	Overall efficiency of reaction	Tabrizi et al 2015

Table A.8: Gas Turbine Combined Cycle

Variable	Min	Max	Units	Description	Source
Turbine efficiency	65	70	%	Overall Electrical Energy out over the LHV of fuel in	https://www.energy.gov/fe/how-gas-turbine-power-plants-work

Table A.9: Steam Turbine

Variable	Min	Max	Units	Description	Source
Turbine efficiency	10	37	%	Electrical Energy out over the heat energy in	https://www.turbinesinfo.com/steam-turbine-efficiency/

Table A.10: Solid Oxide Electrolysis

Variable	Min	Max	Units	Description	Source	Source 2
H_2 ratio	2		%molH_2 / %molCO	Molar ratio of H_2 to CO		
T	1073	1273	K		Ni et al 2007	
delta S	0.163		Kj/mol-K	Change in Entropy of reaction		
Energy of Reaction	285.83		Kj/mol	Total Molar specific energy of reaction		
O2 to H2 ratio	0.5		mol/mol	Molar ratio of Oxygen to Hydrogen in reaction	Carmo et Al	
Specific energy	3.1	3.7	kwh/Nm^3	Specific Energy of H2 production	Udagawa et al 2007	Sunfire

Table A.11: Fischer-Tropsch Synthesis

Variable	Min	Max	Units	Description	Source
alpha	0.8	0.95	NaN	Typical Cobalt-Catalyst LTFT	P. Chaumette et Al 1995
Specific Energy FT	-11195		KJ/kg	Mass specific Heat released during reaction	P. Chaumette et Al 1995
H2 ratio	2		%molH2/%molCO	Molar ratio of H2 to CO	
Max chain	50		# of Carbon	The maximum carbon chain length we care about	
H2O ratio	0.642		kg/kg	The amount of water produced per kg of CO	
T	473.15	523.15	K	Normal Operating Temperature	P. Chaumette et Al 1995
P	1	3	Mpa	Normal Operating Pressure	P. Chaumette et Al 1995

Table A.12: CO_2 Removal

Variable	Min	Max	Units	Description	Source
Separation efficiency	0.99		%	Removal Efficiency of CO2	
Specific Energy of CO_2 removal	23	35	KJ/mol	Specific Energy of CO2 removal	House et al 2011- Appendix Table S3

Table A.13: CO_2 Capture

Variable	Min	Max	Units	Description	Source	Source 2
Flue Gas Seperation						
Flue gas 2nd law efficiency	19	25	%	Wmin/Wactual for seperating substance	House et al 2011	
Specific Energy Flue Gas Seperation	28	35	Kj/molCO2	energy cost per mol of CO2 we want	House et al 2011 - Appendix Table S3	
Direct Air Capture						
DAC 2nd law efficiency	5	9	%	Wmin/Wactual for seperating substance	House et al 2011	Keith et Al 2018
Minimum Work Req	20		kj/molCO2	MINIMUM energy cost per mol CO2 we want	House et al 2011	

Appendix B

Lifecycle Analysis Assumptions

Table B.1: Fuel Specifications

Variable	Value	Units	Description	Source
BTU_to_MJ	948	BTU/MJ		GREET 2017
Gasoline_Density	2.836	kg/gal		GREET 2017
Diesel_Density	3.017	kg/gal		GREET 2017
Gasoline_LHV	41.73	MJ/kg		GREET 2017
Diesel_LHV	43.24	MJ/kg		GREET 2017
Gasoline_c_ratio	0.83	fraction by weight		GREET 2017
Diesel_c_ratio	0.85	fraction by weight		GREET 2017

Table B.2: Upstream Emissions

Variable	Value	Units	Description	Source
Switchgrass Farming	82.11			GREET 2017
Switchgrass Transportation	93.87			GREET 2017
Willow Farming	40.07	gCO2e/kg	GHG-100 Emissions per kg of Willow	GREET 2017
Willow Transportation	55.61	gCO2e/kg	GHG-100 Emissions per kg of Willow	GREET 2017
Miscanthus Farming	46.27	gCO2e/kg		GREET 2017
Miscanthus Transportation	75.48	gCO2e/kg		GREET 2017
Poplar Farming	61.97	gCO2e/kg		GREET 2017
Poplar Transportation	14	gCO2e/kg		GREET 2017
Switchgrass Water Consumption	724.41	cm^3/kg	Water Consumption during farming	GREET 2017
Willow Water Consumption	66.88	cm^3/kg	Water Consumption during farming	GREET 2017
Miscanthus Water Consumption	560000	cm^3/kg	Water Consumption during farming	GREET 2017

Table B.3: GREET 2017 Fuel Properties

Fuel Property	Value	Units	Description	Source
Gasoline_LHV	41.73869935	MJ/kg	LHV	GREET 2017
Diesel_LHV	43.24785345	MJ/kg	LHV	GREET 2017
Gasoline_Density	2.835	kg/gal		GREET 2017
Diesel_Density	3.167	kg/gal		GREET 2017

Table B.4: GREET 2017 Emissions Inventory for Fuel Combustion

	Diesel Avg	Units	Gasoline Avg	Units
CO2 Total	3187.508438	g	2726.55553	g
CO2	3187.508438	g	2726.55553	g
CO2_Biogenic	0	g	0	g
VOC	0.551363335	g	15.65729941	g
CO	8.631769713	g	166.5689436	g
NOx	25.2458725	g	7.238128563	g
PM10	1.253752351	g	1.193770996	g
PM2.5	1.047766463	g	1.18912225	g
SOx	0.022217272	g	0.048955208	g
CH4	0.072383538	g	0.129955366	g
N2O	0.032431692	g	0.033679687	g
BC	0	g	0	g
POC	0	g	0	g

Table B.5: GREET 2017 Fischer-Tropsch Diesel Emissions

Emissions per kg of Fischer-Tropsch Diesel		
Well to Use		
Emissions	FTD	Units
CO2 Total	0.15	kg
CO2	0.15	kg
CO2_Biogenic	-4.97E-04	kg
VOC	0.29	g
CO	0.57	g
NOx	1.71	g
PM10	0.14	g
PM2.5	98.1	mg
SOx	1.69	g
CH4	0.68	g
N2O	0.83	g
BC	17.4	mg
POC	12.83	mg

Appendix C

Techno-economic Analysis Assumptions

Table C.1: Financial Assumptions

Financial Assumptions		
Equity	0.2	Equity
Loan_Interest	0.1	Loan Interest
Loan_Term	10	Loan Term, years
WC	0.05	Working Capital (prop of FCI)
General_Plant	200	General Plant
DPY	10	Depreciation Period (Years)
CPY	3	Construction Period (Years)
CY_1	0.08	Prop Spent in Year -3
CY_2	0.6	Prop Spent in Year -2
CY_3	0.32	Prop Spent in Year -1
WACC	0.15	Discount Rate
ITR	0.169	Income Tax Rate
HPY	8400	Operating Hours per Year
VPY	20	Valuation Period (Years)
Inflation	0 02	Inflation [%/yr]
OPD	350	Operating days
DOC	0.077	Prop of FCI
Prod_Capacity1	0.75	50% in the first 6 months and 100% rest of yr1
Prod_Capacity2	1	100% from year 2 onwards

Table C.2: Process Unit Capital Costs

Process Name	Equipment Cost (EC) (m$ 2016)	EC ref 2	S ref	S ref Units	di	Description	Source 1	Source 2
CO2 Capture	409.7	574.2	2900	tCO2/day	1		Keith et al 2018	
Flue Gas Capture	117.29		8000	tCO2/day	1		DAC Report 2011	
Co-Electrolysis	0.999	3.33	1	MW	1		Schmidt et al 2017	Sunfire GmBH
Compress	0.61		413	kW	0.8	power consumption	Albrecht et al 2017	
Gasifier	100.71	129.6	78	t/h (slurry input)	0.7	slurry input	Worley & Yale 2012	Albrecht et al 2017
Electrolyzer	0.80		1	MW	1	installed capacity	Albrecht et al 2017	
Gas/Liquid Separator	0.11		10	m	0.79	unit length	Albrecht et al 2017	
FT Synth	22.12		208	m^3	1	reactor volume	Albrecht et al 2017	
Hydro	9.74		1.13	kg/s	0.7	feed mass flow	Albrecht et al 2017	
PSA	7.37		0.294	kmol/s	0.74	purge gas flow	Albrecht et al 2017	
RWGS	3.00		2556	t/day	0.65	total mass flow	Albrecht et al 2017	
Selexol Unit	74.41		9909	kmol/h	0.7	CO2 in feed	Albrecht et al 2017	
Steam Turbine	0.43		10.5	MW	0.44	Power output	Albrecht et al 2017	
Gas Turbine	10.59		25	MW	0.7	power output	Albrecht et al 2017	
WGS Reactor	3.48		150	kg/s	0.67	total gas feed	Albrecht et al 2017	

Table C.3: Indirect Capital Costs

Indirect Cost items	j	Basis	Typical Value	Source 1
Total direct plant costs (D)				
Equipment installataion	1	EC	0.47	Albrecht et al 2017
Instrumentation and control	2	EC	0.36	Albrecht et al 2017
Piping (installed)	3	EC	0.68	Albrecht et al 2017
Electrical (installed)	4	EC	0.11	Worley & Yale 2012
Buildings including services	5	EC	0.18	Albrecht et al 2017
Yard Improvements	6	EC	0.1	Albrecht et al 2017
Service Facilities (installed)	7	EC	0.55	Albrecht et al 2017
Total Indirect plant costs (i)				
Engineering and supervison	8	EC	0.33	Albrecht et al 2017
Construction Expenses	9	EC	0.42	Albrecht et al 2017
Legal Expenses	10	EC	0.04	Albrecht et al 2017
As function of (D +I)				
Contractor's Fee	11	D + I	0.05	Albrecht et al 2017
Contingency	12	D + I	0.1	Albrecht et al 2017

Table C.4: Raw Material Costs

Raw Materials & Byproducts	Market Price ($ 2016)	Market Price 2 ($ 2016)	Units	Description	Source 1
Water	0	3.52	$/ton	Water for electrolysis	Brynolf et al 2018
Selexol	5502.57		$/t	1.05E-5 kg/kg biomass	Albrecht et al 2017
Biomass	121.8		$/t		Albrecht et al 2017
Elec_Consumed	131.3		$/MWh		
Elec_Produced	73.16	170.83	$/MWh		
CaCO3	40	340	$/ton CaCO3	Direct Air Capture chemical. 0.0156 kgCaCO3/kgCO2	Alibaba Search, 11/1/2018 ()

Table C.5: Indirect Operating Costs

Investment Item	Basis	Typical Value 1	Value 2	Notes
Operating Supervision	OL	0.15		
Maintenance Labor	FCI	0.01	0.03	
Maintenance material	FCI	0.01	0.03	
Operating supplies	M	0.15		
Laboratory charges	OL	0.2		
Insurance and taxes	FCI	0.02		
Plant Overhead Costs	TLC	0.6		
Administrative Costs	PO	0.25		
Distribution and Selling costs	NPC	0.06		won't be considered
Research and Development costs	NPC	0.04		won't be considered

Appendix D

Power Generation Values

Table D.1: Electricity Generation Emission Indices - NREL Futures Study 2012

Electricity Generation Source	Emission Intensity [gCO2e/kWh]
Coal	980
Natural Gas-CT	670
Natural Gas-CC	487
Petroleum	840
Nuclear	12
Hydropower	7
Biomass	40
Geothermal	37
PV-Rooftop	45
PV-Utility	45
CSP	21
Wind-Onshore	11
Wind-Offshore	11

Table D.2: Electricity Generation Capital Costs by Capacity

Process Name	Capacity Factor (CF) 1	CF 2	Source 1	Source 2
PV	0.21	0.26	Tidball et al., 2010	Tidball et al., 2010
Solar Thermal	0.32	0.36	Tidball et al., 2010	Tidball et al., 2010
Wind (onshore)	0.42	0.44	Tidball et al., 2010	Tidball et al., 2010
Wind (offshore)	0.40	0.45	Tidball et al., 2010	Tidball et al., 2010
Geothermal	0.85	0.97	Tidball et al., 2010	Tidball et al., 2010
Nuclear	0.90	0.9	Tidball et al., 2010	Tidball et al., 2010

Table D.3: Electricity Generation Capacity Factors

Process Name	Min. Capital	Max Capital	Units	Source 1	Source 2
PV	1856	2165	$/kW	Tidball et al., 2010	Tidball et al., 2010
Solar Thermal	2990	4949	$/kW	Tidball et al., 2010	Tidball et al., 2010
Wind (onshore)	1031	2320	$/kW	Tidball et al., 2010	Tidball et al., 2010
Wind (offshore)	1547	2320	$/kW	Tidball et al., 2010	Tidball et al., 2010
Geothermal	2268	3918	$/kW	Tidball et al., 2010	Tidball et al., 2010
Nuclear	3093	4124	$/kW	Tidball et al., 2010	Tidball et al., 2010

Table D.4: On-Site Generation Results Summary Table

Pathway	Generation Source	Electricity Emissions Index (gCO2e/kWh)	Average Fuel Emissions [gCO2e/MJ]	CAPEX ($MM 2016)	MSP ($/L)
BtL	Wind	11	23	276	1.51
PBtL	Wind	11	16	1157	1.18
PtL_ElecRWGS	Wind	11	8	2448	1.92
PtL_CoElec	Wind	11	7	2816	2.04
BtL	PV	45	23	276	1.51
PBtL	PV	45	28	2224	1.84
PtL_ElecRWGS	PV	45	35	4748	3.39
PtL_CoElec	PV	45	28	4657	3.20
BtL	Geothermal	37	23	276	1.51
PBtL	Geothermal	37	25	1192	1.20
PtL_ElecRWGS	Geothermal	37	29	2524	1.97
PtL_CoElec	Geothermal	37	23	2877	2.08
BtL	Nuclear	12	23	276	1.51
PBtL	Nuclear	12	16	1321	1.28
PtL_ElecRWGS	Nuclear	12	9	2801	2.14
PtL_CoElec	Nuclear	12	7	3094	2.22

Bibliography

[1] Intergovernmental Panel on Climate Change. *Global warming of 1.5°C.* 2018. OCLC: 1056192590.

[2] Friedemann Georg Albrecht, Daniel Helmut Konig, Nadine Baucks, and Ralph-Uwe Dietrich. A standardized methodology for the techno-economic evaluation of alternative fuels: A case study. *Fuel*, 194:511–526, April 2017.

[3] Albert R. Gnadt, Raymond L. Speth, Jayant S. Sabnis, and Steven R. H. Barrett. Technical and environmental assessment of all-electric 180-passenger commercial aircraft. *Progress in Aerospace Sciences*, 105:1–30, February 2019.

[4] M Grahn, M Taljegard, and S Brynolf. Electricity as an Energy Carrier in Transport: Cost and Efficiency Comparison of Different Pathways. *Conference Proceedings*, page 7, 2018.

[5] ICAO Environmental Report 2016: Aviation and Climate Change. Technical report, ICAO, 2016.

[6] James I Hileman, David S Ortiz, James T Bartis, Hsin Min Wong, Pearl E Donohoo, Malcolm A Weiss, and Ian A Waitz. Near-Term Feasibility of Alternative Jet Fuels. page 152.

[7] Mark D. Staples, Robert Malina, Hakan Olcay, Matthew N. Pearlson, James I. Hileman, Adam Boies, and Steven R. H. Barrett. Lifecycle greenhouse gas footprint and minimum selling price of renewable diesel and jet fuel from fermentation and advanced fermentation production technologies. *Energy & Environmental Science*, 7(5):1545–1554, April 2014.

[8] Mark Douglas Staples. Bioenergy and its use to mitigate the climate impact of aviation. page 170.

[9] Iva Ridjan, Brian Vad Mathiesen, and David Connolly. Terminology used for renewable liquid and gaseous fuels based on the conversion of electricity: a review. *Journal of Cleaner Production*, 112:3709–3720, January 2016.

[10] Selma Brynolf, Maria Taljegard, Maria Grahn, and Julia Hansson. Electrofuels for the transport sector: A review of production costs. *Renewable and Sustainable Energy Reviews*, 81:1887–1905, January 2018.

[11] Daniel H. Konig, Marcel Freiberg, Ralph-Uwe Dietrich, and Antje Warner. Techno-economic study of the storage of fluctuating renewable energy in liquid hydrocarbons. *Fuel*, 159:289–297, November 2015.

[12] Andrea Konig, Kirsten Ulonska, Alexander Mitsos, and Jorn Viell. Optimal Applications and Combinations of Renewable Fuel Production from Biomass and Electricity. *Energy & Fuels*, 33(2):1659–1672, February 2019.

[13] Herib Blanco, Wouter Nijs, Johannes Ruf, and Andre Faaij. Potential for hydrogen and Power-to-Liquid in a low-carbon EU energy system using cost optimization. *Applied Energy*, 232:617–639, December 2018.

[14] Laura E. Hombach, Larissa DorÃČÂľ, Katrin Heidgen, Heiko Maas, Timothy J. Wallington, and Grit Walther. Economic and environmental assessment of current (2015) and future (2030) use of E-fuels in light-duty vehicles in Germany. *Journal of Cleaner Production*, 207:153–162, January 2019.

[15] Andrea Monti, Lorenzo Barbanti, Alessandro Zatta, and Walter Zegada-Lizarazu. The contribution of switchgrass in reducing GHG emissions. *GCB Bioenergy*, 4(4):420–434, 2012.

[16] Navid Seifkar, Xiaoming Lu, Mitch Withers, Robert Malina, Randall Field, Steven Barrett, and Howard Herzog. Biomass to Liquid Fuels Pathways: A Techno-Economic Environmental Evaluation. Technical report, MIT Energy Initiative, 2015.

[17] Xiangmei Meng, Wiebren de Jong, Ningjie Fu, and Adrian H.M. Verkooijen. Biomass gasification in a 100 kWth steam-oxygen blown circulating fluidized bed gasifier: Effects of operational conditions on product gas distribution and tar formation. *Biomass and Bioenergy*, 35(7):2910–2924, July 2011.

[18] David W. Keith, Geoffrey Holmes, David St Angelo, and Kenton Heidel. A Process for Capturing CO2 from the Atmosphere. *Joule*, 0(0), June 2018.

[19] World-first Climeworks plant: Capturing CO_2 from air to boost growing vegetables, May 2017.

[20] K. Z. House, A. C. Baclig, M. Ranjan, E. A. van Nierop, J. Wilcox, and H. J. Herzog. Economic and energetic analysis of capturing CO2 from ambient air. *Proceedings of the National Academy of Sciences*, 108(51):20428–20433, December 2011.

[21] Mark E Dry. The Fischer-Tropsch process: 1950-2000. *Catalysis Today*, page 15, 2002.

[22] Morten Thomas Emhjellen. A gas to liquid Fischer-Tropsch process integrated with Solar Thermal Water Split. Master's thesis, Norwegian University of Science and Technology, 2016.

[23] M.A. Laguna-Bercero. Recent Advances in high temperature electrolysis using solid oxide fuel cells: A review. *Journal of Power Sources*, 203:4–16, April 2012.

[24] M Ni, M Leung, and D Leung. Technological development of hydrogen production by solid oxide electrolyzer cell (SOEC). *International Journal of Hydrogen Energy*, 33(9):2337–2354, May 2008.

[25] J. Udagawa, P. Aguiar, and N. P. Brandon. Hydrogen production through steam electrolysis: Model-based dynamic behaviour of a cathode-supported intermediate temperature solid oxide electrolysis cell. *Journal of Power Sources*, 180(1):46–55, May 2008.

[26] Qingxi Fu, Corentin Mabilat, Mohsine Zahid, Annabelle Brisse, and Ludmila Gautier. Syngas production via high-temperature steam/CO 2 co-electrolysis: an economic assessment. *Energy & Environmental Science*, 3(10):1382–1397, 2010.

[27] Gregor Herz, Erik Reichelt, and Matthias Jahn. Techno-economic analysis of a co-electrolysis-based synthesis process for the production of hydrocarbons. *Applied Energy*, 215:309–320, April 2018.

[28] K. Hauptmeier, Personal Communication, June 4, 2018.

[29] Mitch R. Withers, Robert Malina, Christopher K. Gilmore, Jonathan M. Gibbs, Chris Trigg, Philip J. Wolfe, Parthsarathi Trivedi, and Steven R. H. Barrett. Economic and environmental assessment of liquefied natural gas as a supplemental aircraft fuel. *Progress in Aerospace Sciences*, 66:17–36, April 2014.

[30] Power-to-Liquids: Potentials and Perspectives. Technical report, German Environment Agency, September 2016.

[31] NREL Renewable Futures Study: Executive Summary. Data file, National Renewable Energy Laboratory, 2012.

[32] Matthew Pearlson, Christoph Wollersheim, and James Hileman. A techno-economic review of hydroprocessed renewable esters and fatty acids for jet fuel production. *Biofuels, Bioproducts and Biorefining*, 7(1):89–96, January 2013.

[33] Seamus J. Bann, Robert Malina, Mark D. Staples, Pooja Suresh, Matthew Pearlson, Wallace E. Tyner, James I. Hileman, and Steven Barrett. The costs of production of alternative jet fuel: A harmonized stochastic assessment. *Bioresource Technology*, 227:179–187, March 2017.

[34] United States Environmental Protection Agency. eGRID Summary Tables 2016, February 2018.

[35] Lifecycle greenhouse gas emissions for select pathways. Data and Tools, United States Environmental Protection Agency, July 2016.

[36] D. Keith Personal Communication, October 23, 2018.

[37] R Tidball, J Bluestein, N Rodriguez, S Knoke, ICF International, and J Macknick. Cost and Performance Assumptions for Modeling Electricity Generation Technologies. *Renewable Energy*, page 211, 2010.

[38] 2016 billion-ton report: Advancing domestic resources for a thriving bioeconomy, volume 1: Economic availability of feedstocks. Data file, United States Department of Energy.

[39] Patrick Insinger David W. Keith Francis M. O' Sullivan Dharik S. Mallapragada, Emre Gencer. Cost-Effectiveness of Continuous H_2 Production from Integrated PV-Electrolysis-Storage Systems. *In Preparation*, 2019.

[40] Annual Energy Outlook 2018 with Projections to 2050. Data file, United States Energy Information Administration.

[41] Kenneth Gillingham and James H. Stock. The Cost of Reducing Greenhouse Gas Emissions. *Journal of Economic Perspectives*, 32(4):53–72, 2018.